



**UNIVERSITY OF LEEDS**

This is a repository copy of *Syn-metamorphic folding in the Tauern Window, Austria dated by Th-Pb ages from individual allanite porphyroblasts*.

White Rose Research Online URL for this paper:

<http://eprints.whiterose.ac.uk/85153/>

Version: Accepted Version

---

**Article:**

Cliff, RA, Oberli, F, Meier, M et al. (2 more authors) (2015) Syn-metamorphic folding in the Tauern Window, Austria dated by Th-Pb ages from individual allanite porphyroblasts. *Journal of Metamorphic Geology*, 33 (4). 427 - 435. ISSN 0263-4929

<https://doi.org/10.1111/jmg.12127>

---

**Reuse**

Unless indicated otherwise, fulltext items are protected by copyright with all rights reserved. The copyright exception in section 29 of the Copyright, Designs and Patents Act 1988 allows the making of a single copy solely for the purpose of non-commercial research or private study within the limits of fair dealing. The publisher or other rights-holder may allow further reproduction and re-use of this version - refer to the White Rose Research Online record for this item. Where records identify the publisher as the copyright holder, users can verify any specific terms of use on the publisher's website.

**Takedown**

If you consider content in White Rose Research Online to be in breach of UK law, please notify us by emailing [eprints@whiterose.ac.uk](mailto:eprints@whiterose.ac.uk) including the URL of the record and the reason for the withdrawal request.



[eprints@whiterose.ac.uk](mailto:eprints@whiterose.ac.uk)  
<https://eprints.whiterose.ac.uk/>

Received Date : 24-Sep-2014  
Revised Date : 02-Feb-2015  
Accepted Date : 09-Feb-2015  
Article type : Original Article

## **Syn-metamorphic folding in the Tauern Window, Austria dated by Th-Pb ages from individual allanite porphyroblasts.**

R.A. Cliff<sup>1</sup>, F. Oberli<sup>2</sup>, M. Meier<sup>2</sup>, G.T.R. Droop<sup>3</sup> and M.Kelly<sup>1</sup>

<sup>1</sup>Institute of Geophysics and Tectonics, School of Earth and Environment, University of Leeds, Leeds, LS2 9JT, UK

<sup>2</sup>Institute of Geochemistry and Petrology, ETH Zurich, CH-8092 Zurich, Switzerland

<sup>3</sup>School of Earth, Atmospheric & Environmental Sciences, University of Manchester, Oxford Road, Manchester, M13 9PL, UK

Short title: Allanite Th-Pb age of syn-metamorphic folding

### **Abstract**

High-precision <sup>232</sup>Th-<sup>208</sup>Pb dates have been obtained from allanite porphyroblasts that show unambiguous microstructural relationships to fabrics in a major syn-metamorphic fold in the SE Tauern Window, Austria. Three porphyroblasts were analysed from a single garnet mica schist from the Peripheral Schieferhülle in the core of the Ankogel Synform, one of a series of folds which developed shortly before the thermal peak of Alpine epidote-amphibolite-facies metamorphism: allanite grain 1 provided two analyses with a combined age of  $27.7 \pm 0.7$  Ma; grain 2, which was slightly bent and fractured during crenulation, provided two analyses with a combined age of  $27.7 \pm 0.4$  Ma; a single analysis from grain 3, which overgrew an already crenulated fabric, gave an age of  $28.0 \pm 1.4$  Ma. The five <sup>232</sup>Th-<sup>208</sup>Pb ages agree within error and define an isochron with an age of  $27.71 \pm 0.36$  Ma (95% c.l.; MSWD = 0.45). The results imply that the crenulation event was in progress in a short interval (<1 Ma) around 28 Ma and that the Ankogel Synform was forming at this time. The thermal peak of regional metamorphism in the SE Tauern Window was probably attained shortly after 28 Ma, only *c.* 5 Ma after eclogite facies metamorphism in the central Tauern Window.

Metasediment may contain allanite porphyroblasts with clear-cut microstructural relationships to fabric development and metamorphic crystallization; for such rocks, <sup>232</sup>Th-<sup>208</sup>Pb dating on microsamples offers a powerful geochronological tool.

Keywords: allanite, Tauern Window, U-Th-Pb geochronology

### **INTRODUCTION**

Determining accurate age information on the thermal and tectonic evolution of metamorphic belts requires both precise analytical techniques and thorough understanding of the relationship between the dated material and the metamorphic crystallization history. Achieving both simultaneously has proved difficult: the most precise analytical data comes from the U-Th-Pb system but generally from minerals which cannot be easily linked by petrographic observation to metamorphic and deformation history, or from minerals where

This article has been accepted for publication and undergone full peer review but has not been through the copyediting, typesetting, pagination and proofreading process, which may lead to differences between this version and the Version of Record. Please cite this article as doi: 10.1111/jmg.12127

This article is protected by copyright. All rights reserved.

there is doubt whether the observed isotope systematics relate to the minerals analysed or to U-Th rich inclusions they contain. These problems were reviewed by Vance *et al.* (2003) and some success in overcoming them using inclusions and rare-earth chemistry has been reported by Rubatto *et al.* (2011) for example. However the link to textural relationships among the major minerals is generally unclear. In this study we present an example where the textures of individual allanite porphyroblasts have clear textural relationships to the crystallization and deformation history of their matrix coupled with Th-Pb isotope systematics that allow precise dating of a specific deformation that produced major folding in the Pennine Zone of the Eastern Alps. The results emphasize the tight timeframe for the thermal evolution from high-*P*/low-*T* conditions to the metamorphic peak.

## GEOLOGICAL SETTING AND PETROGRAPHY

Pennine Zone rocks are exposed in the Tauern Window whose general tectonic setting and the location of the sampling area within it are shown in Fig. 1a. The Ankogel Synform is a major structure developed in Mesozoic cover rocks (Peripheral Schieferhülle) in the SE part of the Tauern Window. It is the most easterly of a fan-shaped array of major asymmetric folds on the west side of the Hochalm-Ankogel massif, a dome cored by Hercynian and older basement orthogneisses (Zentralgneis) and paragneisses (Inner Schieferhülle) (Fig. 1b). These folds, which also include the Hölltor Antiform, Mallnitz Synform and Sonnblick Antiform, are broadly coeval and have been ascribed to the  $D_A^2$  phase of Bickle & Hawkesworth (1978) by Droop (1979), equivalent to D2 of Kurz & Neubauer (1996). They possess W- to SW-dipping axial surfaces, deform older thrust surfaces and a penetrative schistosity ( $S_A^1$ ), and are characterised by an  $S_A^2$  axial-planar crenulation cleavage. The Ankogel Synform is an inclined tight to isoclinal fold that curves around the western flank of the Hochalm-Ankogel Dome (Fig 1). In the vicinity of Mallnitz, the amphibolite that occupies its core forms a rounded hinge with a bulbous outcrop whose width is accentuated by topography; in the mica schists surrounding the amphibolite here, the axial plane is hard to locate precisely, but the axial planes of mesoscopic closed-to-open  $F_A^2$  folds and associated  $S_A^2$  crenulation cleavage dip at  $\sim 30$ - $50^\circ$  to the WSW and  $F_A^2$  fold axes plunge at  $\sim 25$ - $40^\circ$  to the SW. The  $D_A^2$  folding predated the thermal peak of Alpine regional metamorphism as shown by the presence, in many schists, of annealed  $D_A^2$  mica crenulations, locally overgrown by post-tectonic (helicitic) garnet porphyroblasts, and by the observation that the Ankogel Synform is cut by metamorphic isograds (Droop, 1981; Droop & Harte, 1995).

The analysed sample, 53296, is a mica-rich pelitic schist, containing porphyroblasts of garnet and smaller allanite; it occurs low in the Peripheral Schieferhülle, close to the axial trace of the Ankogel Synform. It was collected from Auernigwald, 1.75km NE of Mallnitz at an altitude of 1700m. The pelite is separated from the amphibolite that forms the core of the fold by a thin, up to 20m thick, discontinuous marble band. The full mineral assemblage is: muscovite, garnet, biotite, quartz, allanite, titanomagnetite, apatite, tourmaline, with minor retrograde chlorite. In the fine-grained muscovite-rich matrix,  $S_A^1$  schistosity was extensively crenulated during folding, with some development of new mica parallel to the axial planes of the crenulations (Fig. 2a) which dip at  $48/252$ ; locally, randomly oriented recrystallized muscovite flakes overprint the crenulated schistosity (Fig. 2b).

Euhedral 1.5-2.5 mm diameter garnet porphyroblasts contain fine-grained inclusions generally defining a straight internal schistosity ( $S_A^1$ ) indicating growth before the development of crenulation. Occasional grains have slightly curved inclusion trails near the grain edges. Semi-quantitative chemical data for a typical garnet (Table S1; Fig. S1a) show the garnet is Mn-rich with  $X_{Mn}$  approximately 0.36 in the bulk of the grain. Allanite, typically 0.2-0.3 mm across, contains curved inclusion trails of aligned titanomagnetite. In detail the

Accepted Article

textures indicate porphyroblast growth after original fabric formation and spanning at least part of the period of crenulation development. The inclusion patterns suggest allanite grew toward the end of garnet growth. Figure 2c shows an allanite porphyroblast which has grown over the hinge of a pre-existing crenulation, defined by alignment of titanomagnetite grains. Elsewhere allanite grains are deformed and fractured by the crenulation (Fig. 2d). This texture is closely similar to that of other pelitic schists in the vicinity although allanite in some cases clearly pre-dates the crenulations. The mineral assemblage of the sample itself does not provide tight constraints on metamorphic conditions but it is interbedded with pelites containing typical assemblages of the chloritoid-biotite zone mapped by Droop (1981) and further discussed by Droop (1985) and Droop & Harte (1995) who estimated conditions of  $0.7\pm 0.1$  GPa and  $550\pm 10$  °C based on conventional thermobarometry. Textural evidence in the form of the narrow syn-DA2 rims indicates that the garnet porphyroblasts in the studied schist effectively stopped growing during the  $D_A^2$  crenulation event, i.e. before the helicitic garnet in some of the adjacent schists and thus before the thermal peak of metamorphism. The reason for this early cessation of garnet growth is likely to be related to the exhaustion of primary chlorite in this rock given that, in chloritoid-free schists in the Barrovian sequences of the SE Tauern and elsewhere, garnet growth can be attributed to the continuous reaction  $\text{Chl} + \text{Ms} + \text{Qtz} = \text{Grt} + \text{Bt} + \text{H}_2\text{O}$  (Droop, 1981). Chlorite is therefore likely to have been present during formation of the original  $S_A^1$  schistosity (Fig. 6); if the bulk Mg/Fe ratio of the rock were atypically low, chlorite consumption by this reaction could have resulted in exhaustion of chlorite at a relatively low temperature, which would have halted significant garnet growth at that point.

### Allanite Characterisation

Individual allanite porphyroblasts were examined *in situ* by SEM. Selected examples are illustrated in Fig. 3. They exhibit complex zoning patterns comprising three distinct aspects:

- (i) concentric zoning, sometimes with an oscillatory character (Fig. 3 a);
- (ii) sector zoning (Fig. 3b) and
- (iii) fine scale laminar zoning sub-parallel to the titanomagnetite inclusion fabric

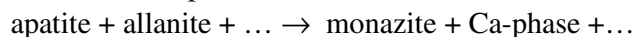
and the external schistosity (Fig. 3c). In part it is defined by discrete rectangular outlines reminiscent of sheet silicate shapes; in some cases their arrangement defines crenulation hinges (Fig.3d) while locally they are randomly orientated, mimicking on a finer scale the decussate textures of some muscovite (Fig.3e). These features are typical of other allanite grains examined including the three analysed grains.

Examination of the chemistry of one porphyroblast in detail using the microprobe confirms that the atomic number contrast in all three zoning styles is mainly related to varying thorium concentration which ranges from  $<1$  to  $>2.5\%$  (Fig. 2f,g). Some of the more subtle effects appear to involve zoning of the light rare earth elements. Partial electron microprobe analyses of a typical grain are presented in Table S2 and Fig. S2.

In addition to inclusions of titanomagnetite and white mica inclusions there are occasional tiny ( $<10\mu\text{m}$ ) inclusions of zircon and monazite, the latter mainly located in cracks. Zoning patterns in the allanite are sharply truncated by these cracks and there is no evidence of allanite recrystallization by later alteration and the continuity of zoning patterns from core to rim indicates they grew in a single metamorphic episode.

The development of new allanite porphyroblasts at this metamorphic grade is interesting as it is well above conditions where allanite usually grows at the expense of detrital monazite and close to conditions where allanite is succeeded by new metamorphic monazite (Smith & Barreiro 1990; Wing *et al.*, 2003; Janots *et al.*, 2008, 2009) although as emphasised by Spear (2010) reactions controlling this isograd are complex and not fully

understood. However apart from minor grossular component in garnet, apatite and allanite are the only calcium-bearing minerals in this rock. Approximate whole rock CaO and Al<sub>2</sub>O<sub>3</sub> contents calculated from modal proportions of minerals are ~0.5 and 25 wt% respectively. Under the metamorphic conditions of the sample published models (Janots *et al.*, 2007; Spear, 2010) suggest reactions with apatite, of the form:



should have occurred in rocks of such low Ca concentrations. The composition of allanite in the present sample differs significantly from the modelled examples; in particular Th contents are much higher, typically 1% and up to 5% of the A-sites are occupied by Th. In addition significant amounts of Mn are also present (~0.1 per formula unit, Table S2). As a consequence the allanite stability field may have expanded to higher temperatures. It is noteworthy that the outermost zones of the analysed garnet have lower Mn (Fig. S1a) which correlates with the timing of allanite growth inferred from the inclusion patterns.

A possible mechanism to explain the nucleation and growth of the allanite porphyroblasts close to the metamorphic peak in this sample would involve the survival of detrital monazite during prograde metamorphism because of the unusually Ca-poor composition of this particular pelite until, at peak conditions, it reacted with Ca, introduced metasomatically from the immediately overlying greenstones and/or carbonates.

### **Pb-isotopic behaviour of allanite**

The value of allanite in geochronology has been emphasized in several recent studies (Gregory *et al.*, 2007; Janots *et al.*, 2008, 2009; Smye *et al.*, 2014). Because of its relatively high closure temperature for Pb isotopic diffusion, allanite is particularly suitable for dating metamorphic crystallization in the present context. Spear & Parrish (1996) confirmed earlier suggestions of a value close to 650°C, and Oberli *et al.* (2004) presented evidence for a value even above 700°C for an igneous system. In either case conditions of allanite crystallization here are well below the closure temperature and allanite ages potentially date crystallization. The excellent preservation of growth zoning features confirms that diffusion of major and trace elements was also limited under these metamorphic conditions.

There are also potential complications with allanite dating. First, because allanite incorporates Th preferentially to U, it also incorporates unsupported <sup>230</sup>Th which by decay leads to enhanced <sup>206</sup>Pb abundances which require correction if ages are based on the <sup>238</sup>U-<sup>206</sup>Pb system (e.g. Schärer, 1984; Oberli *et al.*, 2004). This problem is avoided by using the <sup>232</sup>Th-<sup>208</sup>Pb decay scheme. Second, because metamorphic allanite growth is often linked to monazite breakdown there is a possibility that the initial Pb may be more radiogenic than that in U,Th-poor phases used to estimate the initial Pb (Romer & Siegesmund, 2003). This issue is discussed specifically below. An additional complication is the common presence of small thorite inclusions (Smye *et al.*, 2014), but no evidence of such inclusions was seen during SEM examination of over 50 allanite grains in this study. Furthermore, an often relatively high common lead content in metamorphic allanite (e.g. Gregory *et al.*, 2007) negatively affects age resolution, a problem which is also encountered in the present study.

### **ANALYTICAL METHODS AND RESULTS**

Allanite samples were obtained from polished, 150 µm thick sections after petrographic examination in the SEM (SEM and electron microprobe techniques used are summarised in Appendix S1). Individual allanite porphyroblasts were extracted under the petrographic microscope using a stage-mounted drill. After extraction of the sample plugs, adhering mica-rich matrix was gently scraped off the individual allanite crystals, revealing perfectly flat euhedral crystal faces. Prior to isotopic analysis, the allanite grains were ultrasonically



cleaned in analytical grade hexane, acetone, and high-purity water in order to remove residues from the crystal mounts. Th-U-Pb isotopic measurements were made on five allanite grains, two pairs of fragments of single allanite porphyroblasts and one single grain, following procedures described in Oberli *et al.* (2004). Further analytical details are given in the footnotes to Table 1. Initial Pb isotopic composition was estimated by analysis of a conventional white mica separate from the same hand specimen.

Analytical data for the white mica separate and five allanite microsamples are listed in Table 1. Each allanite yielded approximately 2-5 ng Pb; blanks were less than 1% of the Pb analysed. Th concentrations in allanite range from 8000 to 12000 µg/g, U concentrations are between 500 and 800 µg/g and Pb concentrations between 150 and 220 µg/g. The white mica has a low U/Pb ratio with  $^{238}\text{U}/^{204}\text{Pb}$  of 0.17; the Th/U ratio was determined as  $<2$  using *in situ* LA-ICPMS (see Appendix S1); this confirms that the Th/Pb ratio is low enough that thorogenic Pb growth is insignificant on the 30 Ma timescale. The data are plotted in Fig. 4 which shows a perfect fit to an isochron within analytical error. Hence individual allanite ages were calculated using the white mica analysis as a proxy for initial lead isotopic compositions. The results are plotted on a  $^{208}\text{Pb}/^{232}\text{Th} - ^{206}\text{Pb}/^{238}\text{U}$  concordia diagram in Fig. 5, which also shows SEM images of the analysed grains.

The two halves of grain 1 (Fig. 5) have  $^{232}\text{Th}-^{208}\text{Pb}$  ages of  $27.6\pm 0.9$  and  $27.7\pm 1.1$  Ma while the fractured elongate grain 2 has  $^{232}\text{Th}-^{208}\text{Pb}$  ages of  $27.9\pm 0.6$  and  $27.4\pm 0.7$  Ma. The single analysis of grain 3 gives  $28.0 \pm 1.3$  Ma (errors at the 95% confidence level). The five  $^{232}\text{Th}-^{208}\text{Pb}$  ages agree well within error and taken together define an age of  $27.71\pm 0.36$  Ma (MSWD=0.45, Fig. 3). The corresponding  $^{238}\text{U}-^{206}\text{Pb}$  ages are slightly older and they plot below concordia on the Th-U concordia diagram in Fig 5; as noted above the latter ages are likely to be biased by excess  $^{206}\text{Pb}$  and they are not considered further.

## DISCUSSION

Because of their young age and high common lead concentrations, the calculated ages are sensitive to uncertainties in the composition and uniformity of initial lead. The use of the lead isotopic composition of white mica as the best available estimate of initial lead is justified by consideration of the lead mass balance for this rock: white mica comprises ~ 90 volume% of the rock and the remaining 10% is dominated by quartz and biotite. The only mineral likely to have Pb concentrations greater than white mica is allanite but this comprises much less than 1%. Overall we estimate that mica account for 98% of the Pb in the sample and hence would have dominated the composition of lead incorporated into growing allanite porphyroblasts. Romer & Siegesmund (2003) discussed the possibility that initial lead in allanite may be biased by preferential incorporation of radiogenic lead from monazite breakdown. Given the Pb mass balance and petrographic evidence for active white mica crystallization during allanite growth (Fig. 2), this is unlikely in the present case. For two of the analysed allanite grains two separate fragments of each, with different Th contents, were analysed and the good agreement between them supports this conclusion as does the agreement between the  $^{208}\text{Pb}/^{204}\text{Pb}$  of white mica and the initial  $^{208}\text{Pb}/^{204}\text{Pb}$  ratio of the allanite isochron if the five allanite grains are regressed without the white mica data (Fig.4).

Weighted averages of data for the paired fragments gives ages of  $27.7 \pm 0.7$  Ma for grain 1 and  $27.7 \pm 0.4$  Ma for grain 2. The latter grain was slightly bent and fractured during crenulation (Fig. 5 lower image). In contrast grain 3 overgrew an already slightly crenulated fabric (Fig.5 upper image) but has an indistinguishable age of  $28.0\pm 1.4$  Ma. Thus the crenulation event was in progress in a short interval around 28 Ma. If the dated allanite grains span the whole event then it probably lasted no more than 1 Ma.

The relationship of the allanite age to the overall microstructural evolution of the rock is summarised in the cartoon in Fig. 6 and the link between the microstructures and the mesoscopic folding implies that the Ankogel Synform was actively developing at this time. Peak-metamorphic temperatures were reached at shortly afterwards. The lack of post-metamorphic deformation further implies that folding in the Ankogel Synform was complete by 28 Ma.

Previous geochronological studies of the age of peak metamorphism in the SE Tauern Window have more ambiguous relationships to crystallization history. A study of white mica Rb-Sr ages in the schists from the Mallnitz Synform, 6 km NW of the present study (Inger & Cliff, 1994) found a range of ages from 32 to 23 Ma which they correlated with variations in textural relationships between white mica and fabric development (Fig. 6); samples with well developed crenulation, correlated with formation of the Mallnitz Synform, gave ages of  $28.7 \pm 0.7$  Ma. This is consistent with the assignment of the Mallnitz and Ankogel Synforms to the same  $D_A^2$  episode. On the SW flank of the Sonnblick Antiform, six white mica separates from Gneiss Lamella 4 (Exner, 1964), part of the Rote Wand-Modereck Nappe gave a mean Rb-Sr age of  $27.2 \pm 0.8$  Ma (Reddy *et al.*, 1993). In the core of the Sonnblick Antiform Rb-Sr bulk white mica ages scatter widely but a microsampling study showed white mica crystallization associated with crenulation occurred at  $25.5 \pm 0.3$  Ma (Cliff & Meffan-Main, 2003), implying continued deformation to a later date here. Glodny *et al.* (2008) presented white mica ages suggesting continued ductile deformation in mylonites along the Mölltal Line until 20 Ma. In the SE Tauern Window the earlier parts of the metamorphic  $P$ - $T$  path, including the blueschist facies evidenced by pseudomorphs after lawsonite, remain undated.

Near the southern margin of the central Tauern Window the earlier stages are better dated. Here eclogite facies assemblages have yielded consistent ages  $32.8 \pm 0.5$  Ma by Lu-Hf on garnet (Nagel *et al.*, 2013),  $34.2 \pm 3.6$  Ma by U-Pb on allanite (Smye *et al.*, 2011); white mica Rb-Sr ages on coarse eclogite facies mobilisates are  $31.5 \pm 0.7$  and  $32.1 \pm 1.6$  Ma (Glodny *et al.*, 2005). Tightly grouped white mica Rb-Sr ages between 30.6 and 31.4 Ma (Glodny *et al.*, 2008) date subsequent shearing under greenschist facies conditions within and at the margins of the Eclogite Zone and samples with the best-preserved peak greenschist assemblages range from  $31.3 \pm 0.6$  to  $28 \pm 1$  Ma (Inger & Cliff, 1994 excluding samples with post-peak retrogressive minerals such as biotite). Smye *et al.* (2011) discussed the problems in achieving peak Barrovian metamorphic conditions within a short interval after eclogite formation; they suggest up to 10 Ma for this interval but the latest dating suggests the time scale may be no more than 3 Ma.

In the West Tauern Window, peak amphibolite facies conditions appear to have been reached at a similar time: an Rb-Sr age based on analysis of two garnet rims and nearby matrix indicates an age of  $31 \pm 1$  Ma (Christensen *et al.*, 1994). More recent work indicates that Sr incorporated into growing garnet may often have come from a reservoir that differed from that defined by the matrix at the time of garnet growth (Sousa *et al.*, 2013). However in the Upper Schieferhülle sample analysed by Christensen *et al.* (1994) the matrix was feldspar free and the Sr budget of the matrix is likely to reflect the assemblage from which garnet grew, at least for the garnet rims. One sample dated by Glodny *et al.* (2008) apparently confirms deformation under amphibolite facies conditions occurred at  $31.2 \pm 0.4$  Ma although other samples suggest similar conditions persisted until *c.* 20 Ma.

## CONCLUSIONS

The three allanite grains dated by Th-Pb here provide a precise age of  $27.71 \pm 0.36$  Ma for a texturally well-defined stage close to the metamorphic peak in the SE Tauern Window. Together with recent improved estimates of the timing of eclogite facies metamorphism this

age again emphasises how quickly peak metamorphic conditions were reached after the high pressure stage.

Where metasedimentary rocks contain allanite with clear-cut microstructural relationships to fabric development and metamorphic crystallization,  $^{232}\text{Th}$ - $^{208}\text{Pb}$  dating on microsamples offers a particularly powerful geochronological tool with the potential to resolve the timing of deformation at the <1 Ma level. In other situations where allanite crystallises earlier in the metamorphic history it may provide a means to data stages on the prograde  $P$ - $T$  path.

#### ACKNOWLEDGEMENTS

We are grateful to E. Condliffe for his help with SEM imaging and electron probe analysis of allanite and to R. Walshaw for help with the garnet analysis. L. Forbes assisted with the LA-ICPMS reconnaissance of U/Th ratio in white mica. We are grateful to A. Smye and an anonymous reviewer for their helpful comments on this paper.

#### REFERENCES

- Bickle, M.J. & Hawkesworth, C. J., 1978, Deformation phases and the tectonic history of the Eastern Alps. *Geological Society of America Bulletin*, **89**, 293-306.
- Christensen, J.N., Selverstone, J., Rosenfeld, J.L. & DePaolo, D.J., 1994. Correlation of Rb-Sr geochronology of garnet growth histories from different structural levels within the Tauern Window, Eastern Alps. *Contributions to Mineralogy and Petrology*, **118**, 1-12.
- Cliff, R.A. & Meffan-Main S., 2003. Evidence from Rb-Sr microsampling geochronology for the timing of Alpine deformation in the Sonnblick Dome, SE Tauern Window, Austria, In: Vance, D., Muller, W. & Villa, I.M. (ed.) *Geochronology: linking the isotopic record with petrology and textures. Geological Society, London, Special Publications* **220**, 159-172.
- Droop, G.T.R., 1979. Metamorphic studies in the southeast Tauern Window, Austria. *Unpublished D.Phil thesis, University of Oxford*, 357pp.
- Droop, G.T.R., 1981. Alpine metamorphism of pelitic schists in the south-east Tauern Window, Austria. *Schweizerische Mineralogische und Petrographische Mitteilungen*, **61**, 237-273.
- Droop, G.T.R., 1985. Alpine metamorphism in the southeast Tauern Window, Austria. 1. P-T variations in space and time. *Journal of Metamorphic Geology*, **3**, 371-402.
- Droop, G.T.R. & Harte, B., 1995. The effect of Mn on the phase relations of medium-grade pelites; constraints from natural assemblages on petrogenetic grid topology. *Journal of Petrology*, **36**, 1549-1578.
- Exner, Ch., 1964. Erläuterungen zur Geologischen Karte der Sonnblickgruppe. *Geologische Bundesanstalt, Wien*: 130 pp.
- Glodny, J., Ring, U., Kühn, A., Gleissner, P. & Franz, G., 2005. Crystallization and very rapid exhumation of the youngest Alpine eclogites (Tauern Window, Eastern Alps) from Rb/Sr mineral assemblage analysis. *Contributions to Mineralogy and Petrology*, **149**, 699-712.
- Glodny, J., Ring, U. & Kühn, A., 2008. Coeval high-pressure metamorphism, thrusting, strike-slip, and extensional shearing in the Tauern Window, Eastern Alps, *Tectonics*, **27**, 1-27.
- Gregory, C. J., Rubatto, D., Allen, C., Williams, I. S., Hermann, J. & Ireland, T. R., 2007. Allanite micro-geochronology: a SHRIMP and LA-ICP-MS study. *Chemical Geology*, **245**, 162-182.



- Inger, S. & Cliff, R.A., 1994. Timing of metamorphism in the Tauern Window, Eastern Alps - Rb-Sr ages and fabric formation. *Journal of Metamorphic Geology*, **12**, 695-707.
- Janots, E., Brunet, F., Goffé, B., Poinssot, C., Burchard, M. & Cemič, L., 2007. Thermochemistry of monazite-(La) and dissakisite-(La): implications for monazite and allanite stability in metapelites. *Contributions to Mineralogy and Petrology*, **154**, 1-14.
- Janots, E., Engi, M., Berger, A., Allaz, J., Schwarz, J-O. & Spandler, C., 2008. Prograde metamorphic sequence of REE minerals in pelitic rocks of the Central Alps: implications for allanite–monazite–xenotime phase relations from 250 to 610°C. *Journal of Metamorphic Geology*, **26**, 509–526
- Janots, E., Engi, M., Berger, A., Allaz, J., Schwarz J-O & Spandler, C., 2009. Metamorphic rates in collisional orogeny from in situ allanite and monazite dating. *Geology*, **37**, 11-14.
- Kurz, W. & Neubauer, F., 1996. Deformation partitioning during updoming of the Sonnblick area in the Tauern Window (Eastern Alps, Austria). *Journal of Structural Geology*, **18**, 1327-1343.
- Nagel, T.J., Herwartz, D., Rexroth, S., Münker, C., Froitzheim, N. & Kurz, W., 2013. Lu–Hf dating, petrography, and tectonic implications of the youngest Alpine eclogites (Tauern Window, Austria). *Lithos*, **170–171**, 179–190
- Oberli, F., Meier, M., Berger, A., Rosenberg, C.L. & Gieré, R., 2004. U-Th-Pb and  $^{230}\text{Th}/^{238}\text{U}$  disequilibrium isotope systematics; precise accessory mineral chronology and melt evolution tracing in the Alpine Bergell Intrusion. *Geochimica et Cosmochimica Acta*, **68**, 2543-2560.
- Reddy, S.M., Cliff, R.A. & East, R., 1993. Thermal history of the Sonnblick Dome, south-east Tauern Window, Austria - implications for heterogeneous uplift within the Pennine Basement. *Geologische Rundschau*, **82**, 667-675.
- Romer, R.L. & Siegesmund, S., 2003. Why allanite may swindle about its true age. *Contributions to Mineralogy and Petrology*, **146**, 297-307.
- Rubatto, D., Regis, D., Hermann, J., Boston, K., Engi, M., Beltando, M. & McAlpine, S.R.B., 2011. Yo-yo subduction recorded by accessory minerals in the Italian Western Alps. *Nature Geoscience*, **4**, 338-342.
- Schärer, U., 1984. The effect of initial  $^{230}\text{Th}$  disequilibrium on young U-Pb ages: the Makalu case, Himalaya. *Earth and Planetary Science Letters*, **67**, 191-204.
- Smith, H.A. & Barreiro, B., 1990. Monazite U-Pb dating of staurolite grade metamorphism in pelitic schists. *Contributions to Mineralogy and Petrology*, **105**, 602-615.
- Smye, A.J., Bickle, M.J., Holland, T.J.B., Parrish, R.R. & Condon, D.J., 2011. Rapid formation and exhumation of the youngest Alpine eclogites: A thermal conundrum to Barrovian metamorphism. *Earth and Planetary Science Letters*, **306**, 193–204.
- Smye, A. J., Roberts, N. M., Condon, D. J., Horstwood, M. S. & Parrish, R. R. 2014. Characterising the U–Th–Pb systematics of allanite by ID and LA-ICPMS: Implications for geochronology. *Geochimica et Cosmochimica Acta*, **135**, 1-28.
- Sousa, J., Kohn, M.J., Schmitz, M. D., Northrup C. J. & Spear, F. S., 2013. Strontium isotope zoning in garnet: implications for metamorphic matrix equilibration, geochronology and phase equilibrium modelling. *Journal of Metamorphic Geology*, **31**, 437–452.
- Spear, F.S., 2010. Monazite-allanite phase relations in metapelites. *Chemical Geology*, **279**, 55-62.
- Spear, F.S. & Parrish, R.R., 1996. Petrology and cooling rates of the Valhalla Complex, British Columbia, Canada. *Journal of Petrology*, **37**, 733-765.

Wing, B.A., Ferry, J.M. & Harrison, T.M., 2003. Prograde destruction and formation of monazite and allanite during contact and regional metamorphism of pelites: petrology and geochronology. *Contributions to Mineralogy and Petrology*, **145**, 228-250.

## SUPPORTING INFORMATION

Appendix S1, includes Tables S1 and S2, Figures S1 and S2.

Table S1 Garnet compositions

Table S2 Allanite analyses of grain A48

Figure S1 Typical garnet BSEM image showing straight inclusion trails, a Mn linescan (long white line) and spot analysis locations (white x) in the core, at the edge and 0.1mm from the edge.

Figure S2 BSEM image of allanite A48 from 53296-ii showing the probe analysis locations in relation to zoning. Traverse 1 is approximately normal to the concentric zoning, starting in a 'light' sector (1.1 & 1.2) and continuing in the 'dark' sector. Traverse 3 crosses from the 'light' sector (3.1-3.2) into the 'dark' sector (3.3-3.6)

**Received 24 September 2014; revision accepted 9 February 2015.**

### Figure Captions

**Figure 1** a) General tectonic map of the Tauern Window, showing the location of the detailed map of the study area b) Geological map of part of the SE Tauern Window, after Droop (1979), showing the relationship of the sample locality to the axial trace of the Ankogel Synform (AS). HA: Hölltor Antiform

**Figure 2** Photomicrographs (a) typical area of crenulated schist with porphyroblasts of garnet (G) and allanite (A); note the occurrence of individual white mica grains crystallized parallel to crenulation axial planes, (b) a second area in the same thin section with decussate white mica texture, (c) euhedral allanite porphyroblast overgrowing crenulation defined by titanomagnetite grains. The matrix is predominantly composed of white mica with minor biotite and titanomagnetite, (d) an elongate allanite grain that has fractured during crenulation.

**Figure 3** Back-scattered SEM images of selected allanite grains showing different styles of zoning. (a) oscillatory zoning, (b) sector zoning, (a,b and c) zoning parallel to schistosity, (d) zoning reflecting allanite replacement of a crenulated schistosity, (e) zoning reflecting allanite replacement of a decussate sheet silicate texture, (f,g) images of a small part of an allanite grain comparing the the back-scattered SEM image (f) and the Th x-ray image of the same area (g) confirming that thorium variation is a major cause of the observed.

**Figure 4**  $^{208}\text{Pb}$ - $^{232}\text{Th}$  isochron plot of the five allanite analyses plus white mica; the latter is not resolved from the y-axis at this scale.

**Figure 5** U-Th concordia diagram showing the similar displacement of all five allanite analyses to the right of concordia due to excess  $^{206}\text{Pb}$  from incorporation of  $^{230}\text{Th}$ . The insets show BSEM images of the three analysed grains.

**Figure 6** A cartoon to illustrate microstructural development in relation to the formation of the the Mallnitz and Ankogel synforms. The upper panel shows the growth of allanite in 53296. The lower panel compares this with the less precise data from the Mallnitz synform to the west.

**Table 1** U, Th and Pb data for minerals from sample 53296 (Leeds registration number; collected by Droop (1979) as GD731g).

**Table 2** U, Th and Pb data for minerals from sample GD731g (Droop, 1979, registered at Leeds as specimen 53296)

| Sample      | Weight [μg] | U [ppm] | Th [ppm]          | Pb <sup>a</sup> [ppm] | <sup>208</sup> Pb/ <sup>206</sup> Pb <sup>a</sup> | <sup>208</sup> Pb/ <sup>204</sup> Pb <sup>a</sup> | <sup>232</sup> Th/ <sup>204</sup> Pb <sup>a</sup> | $\rho^b$<br><sup>208</sup> Pb/ <sup>204</sup> Pb<br>vs.<br><sup>232</sup> Th/ <sup>204</sup> Pb | <sup>208</sup> Pb/ <sup>232</sup> Th <sup>a,c</sup> | <sup>206</sup> Pb/ <sup>238</sup> U <sup>a,c</sup> | $\rho^b$<br><sup>208</sup> Pb/ <sup>232</sup> Th<br>vs.<br><sup>206</sup> Pb/ <sup>238</sup> U | <sup>208</sup> Pb/ <sup>232</sup> Th Age [Ma] | <sup>206</sup> Pb/ <sup>238</sup> U Age [Ma] |
|-------------|-------------|---------|-------------------|-----------------------|---|---|---|---|---|--|--|---|--|
| White mica  |             | 0.09    | <0.2 <sup>d</sup> | 33                    | 2.0874 ± 1  | 38.81 ± 5   | <2  |   |   |  |  |   |  |
| Allanite 1a | 8.0         | 761     | 8121              | 217                   | 2.1575 ± 17                                       | 42.43 ± 7   | 2637 ± 8  | 0.17  | 0.0013 ± 26   | 0.0044 ± 7   | 0.96   | 27.7 ± 0.5                                    | 28.8 ± 0.5                                   |
| Allanite 1b | 9.3         | 700     | 8651              | 204                   | 2.1840 ± 18                                       | 42.92 ± 7   | 2997 ± 8  | 0.17  | 0.0013 ± 23   | 0.0044 ± 7   | 0.98   | 27.6 ± 0.5                                    | 28.9 ± 0.4                                   |
| Allanite 2a | 25.2        | 559     | 12005             | 181                   | 2.3227 ± 19                                       | 45.53 ± 7   | 4853 ± 12   | 0.18  | 0.0013 ± 15   | 0.0046 ± 7   | 0.97   | 27.9 ± 0.3                                    | 29.6 ± 0.5                                   |
| Allanite 2b | 17.8        | 521     | 10676             | 153                   | 2.3273 ± 19                                       | 45.77 ± 9   | 5124 ± 15   | 0.38  | 0.0013 ± 17   | 0.0044 ± 11  | 0.91   | 27.4 ± 0.3                                    | 28.4 ± 0.7                                   |
| Allanite 3  | 25.9        | 689     | 5742              | 186                   | 2.1192 ± 17                                       | 41.81 ± 7   | 2151 ± 5  | 0.27  | 0.0013 ± 33   | 0.0045 ± 8   | 0.95   | 28.0 ± 0.7                                    | 29.1 ± 0.5                                   |

Allanite analyses were made at ETH Zurich using techniques described by Oberli *et al.* (2004); white mica was analyzed at Leeds using standard chemical techniques and a <sup>202</sup>Pb-<sup>205</sup>Pb double spike.

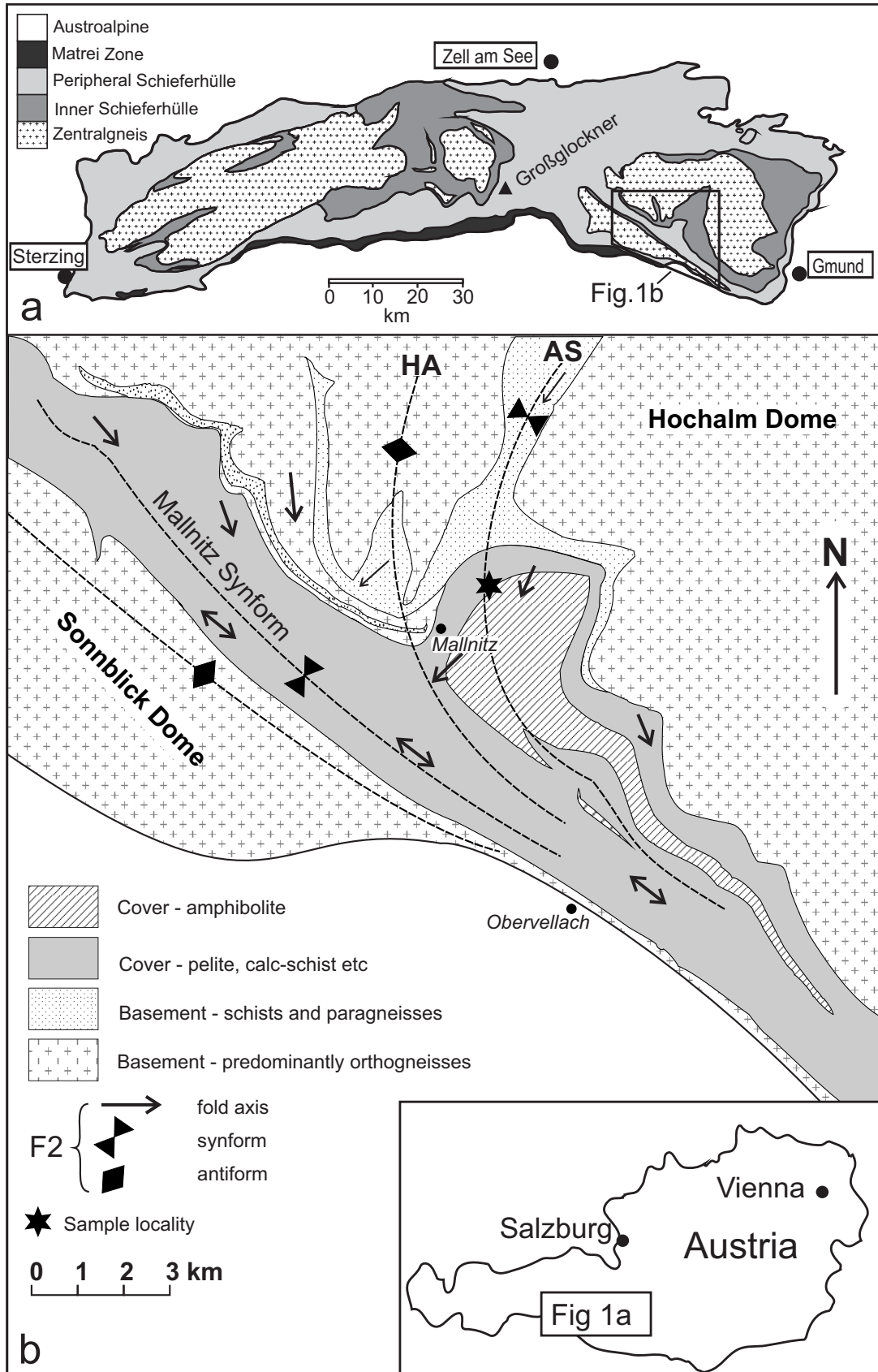
The uncertainties shown are 1σ and for isotope ratios refer to the least significant digits of the corresponding numbers.

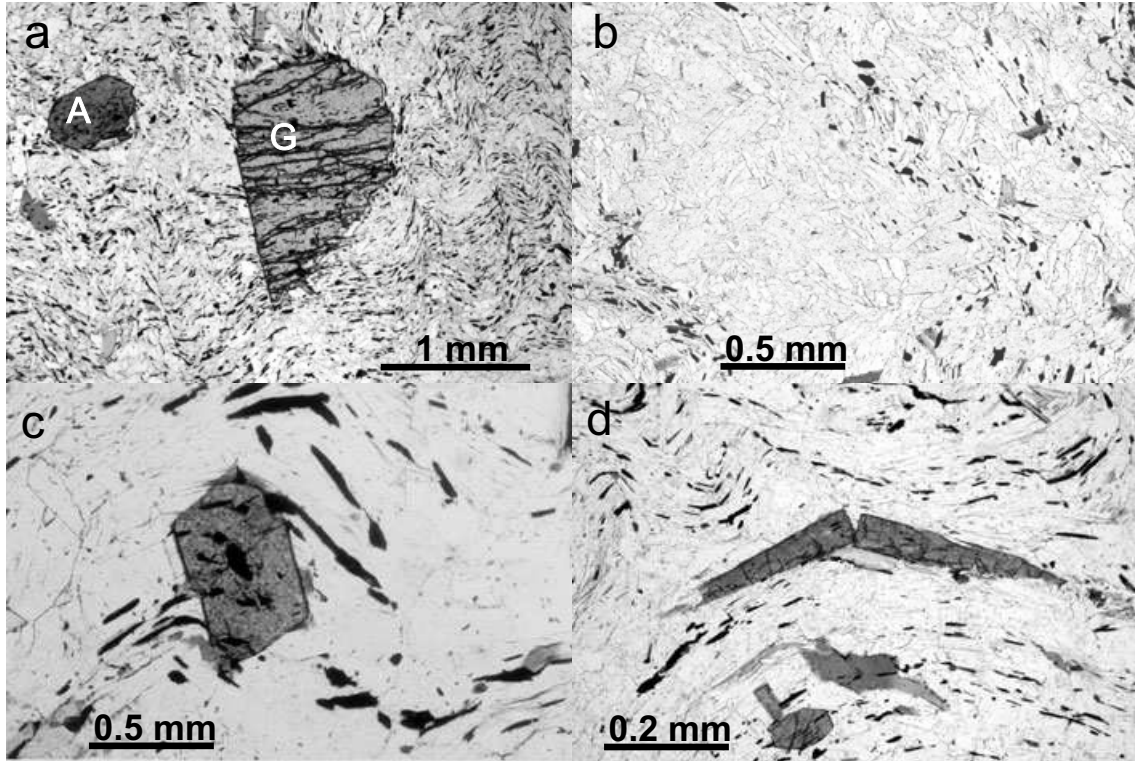
<sup>a</sup> corrected for Pb analytical blank (samples 1a, 1b, 2a: 12.2 ± 3.1 pg; samples 2b, 3: 7.2 ± 2.8 pg; U and Th blanks were negligible) and instrumental mass bias

<sup>b</sup> correlation coefficient

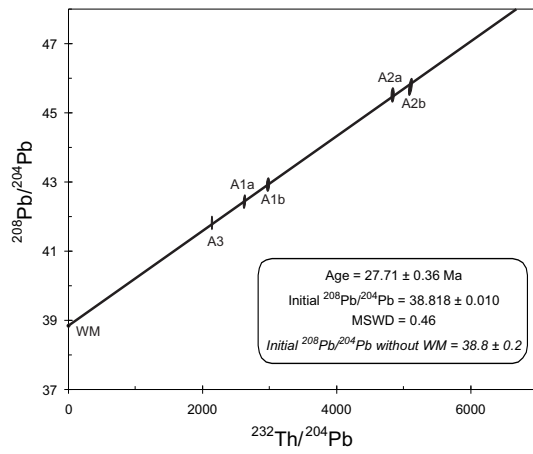
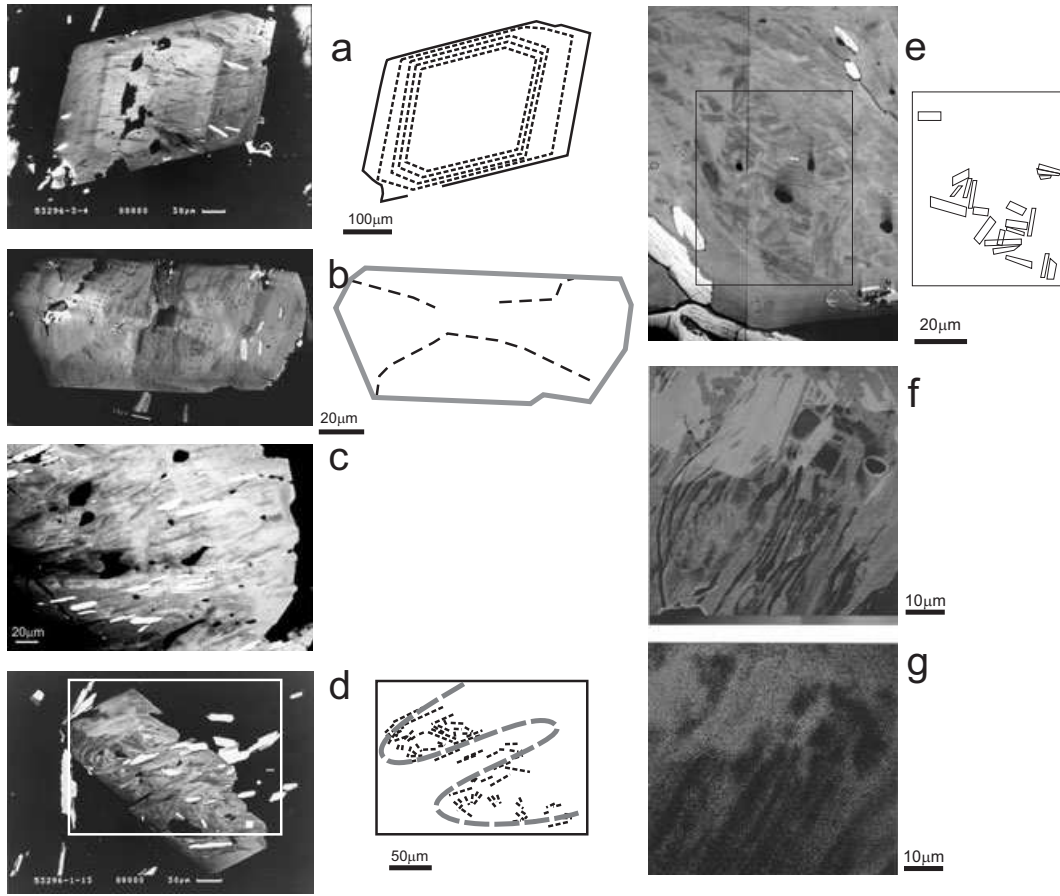
<sup>c</sup> corrected for Pb initially present in the samples using white mica Pb isotopic composition

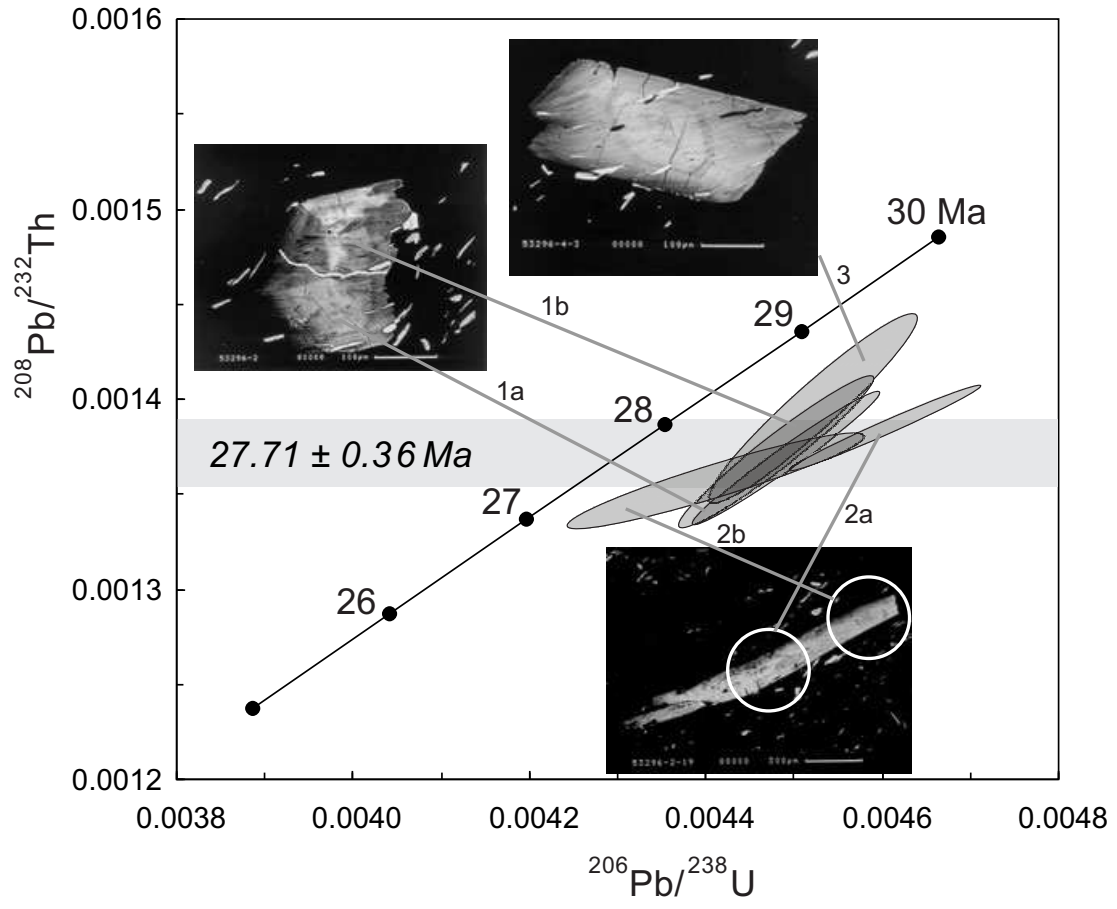
<sup>d</sup> approximate limit on Th concentration in white mica based on LA-ICPMS determination of Th/U ratio (~2)

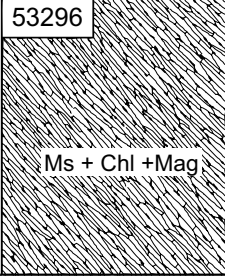
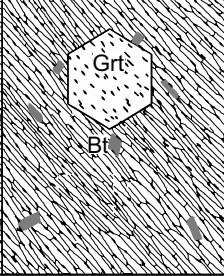
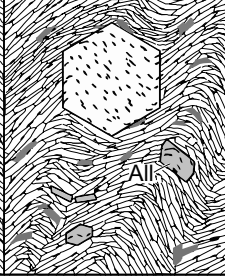
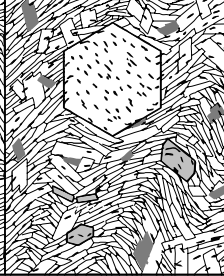
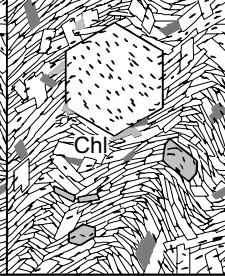










|   |   |  |  |   |
|---|---|--|--|---|
| 53296   |   |  |  |   |
|                |  |   |  |  |
| $D_A^1$   | post- $D_A^1$ pre- $D_A^2$  | $D_A^2$<br>$27.71 \pm 0.36$ Ma   | Metam. Peak  | Retgression   |
| Muscovite & chlorite<br>grow in $S_A^1$ schistosity<br><br>Chl-Ms-Qtz-Mag                       | Garnet & biotite grow<br>Chlorite consumed<br><br>Grt-Bt-Chl-Ms-Qtz-Mag           | Crenulation of schistosity<br>Growth of garnet rims<br>Chlorite exhausted<br>Allanite grows<br><br>Grt-Bt-(Chl)-Ms-Qtz<br>-Mag-All | Decussate micas grow<br><br>Grt-Bt-Ms-Qtz<br>-Mag-All                              | Growth of minor chlorite<br><br>Grt-Bt-Ms-Qtz<br>-Mag-All-Chl                       |
| $\geq 32$ Ma<br>pre-crenulation texture   |   | $28.6 \pm 0.7$ Ma<br>crenulated schists  | $\sim 23$ Ma<br>decussate micas  |   |
| <i>Rb-Sr white mica ages from Mallnitz Synform, ~ 5km W of 53296 - Inger &amp; Cliff (1994)</i> |   |  |  |   |
| Formation of Ankogel<br>and Mallnitz Synforms   |   |  |  |   |